

From atomic to global connectivity in the structure of the SARS-CoV2-Human ACE2 receptor complex

Varsha Subramanyan^{a,(e)}, Arinnia Anto^{b,(c)}, Moitrayee Bhattacharyya^d, Smitha Vishveshwara^a, and Saraswathi Vishveshwara^{b,1}

^aDepartment of Physics, University of Illinois at Urbana-Champaign, Urbana, IL USA; ^bMolecular Biophysics Unit, Indian Institute of Science, Bangalore, Karnataka India; ^cUniversity of Regina, Regina, Saskatchewan, Canada; ^dDepartment of Pharmacology, Yale University, New Haven, CT USA; ^eTheoretical Division, Los Alamos National Laboratory, Los Alamos, NM USA

We investigate connectivity properties of the SARS-CoV2 spike protein-human ACE2-receptor complex employing a protein side chain-based network method that allows us to span a range from atomic to global protein scales. We analyze network topology in terms of clusters and cliques obtained from averaging over snapshots of MD simulations (from D.E. Shaw Research). We demonstrate that SARS-CoV2 forms a more dominant, robust connection with the ACE2-receptor as compared to the less virulent SARS-CoV1. Globally, this stronger connectivity is reflected by our percolation analysis where the interface cluster for the SARS-CoV2-ACE2 complex persists when restricted to stronger and stronger bonds, as compared to the SARSCoV1- ACE2 complex. At the atomic level, interface clique structure reflects a stronger connectivity in the former complex. We pinpoint key functional residues in SARSCoV2 that play important roles in establishing this higher connectivity. Thus, our studies provide an objective method to map spatial connectivity of atomic level non-covalent interactions to global connectivity between any two amino acids in the complex. We also analyze specific snapshots of the MD simulations to highlight prominent variations in network topology that explore diverse conformational landscapes. Finally, we demonstrate that a majority of mutations that occur in the SARSCoV2 spike protein in variants of concern/interest (including the currently circulating JN.1) have been observed at the interface with the ACE2 receptor. Our analyses highlight the importance of interface interactions and provide a rationale for designing receptor-like peptides and proteins to combat immunity-escaping variants.

SARS-CoV2-ACE2 Receptor Interface | Protein Sidechain Network | Global Connectivity Map | Network Analysis

The outbreak of the global COVID-19 pandemic was an unprecedented humanitarian crisis demanding large scale cooperation between governments, scientists and healthcare workers for its alleviation. The Nobel Prizes for Chemistry in 2022 and Medicine in 2023 stand as a testament to the scientific progress made during this period in studying the virus, modelling its spread, understanding its effects and importantly, the development and effective distribution of vaccines. It has encompassed a plethora of experimental, theoretical and computational approaches in a variety of disciplines, including clinical research, immunology, structural and molecular biology, simulations, structural modelling, and network-based analyses. A large body of literature with original research, reviews, and opinions have been generously made available to the public, a few examples of which are referenced here(1–19). However, in spite of the availability of a number of vaccines, the spread of infections and the virulence of SARS-CoV2 variants, continues to be a cause for concern. Mutations in the SARS-

CoV2 spike gene have altered protein binding efficiency and immunogenicity with subsequent lineages leading to variants with higher virulence and/or transmissibility.

The evolutionary trajectory of the virus depends on the complex interplay of a number of factors including the status of vaccination, history of infection, complications in immunocompromised patients etc. It is notable that mutations in variants generally do not occur at single points, instead taking place in multiple locations of the spike protein. A complete understanding of the influence of various factors and such mutations on the functions of the virus- binding efficacy, immunogenicity, and evasive strategies is yet to emerge. A more holistic approach that at once incorporates atomic level interactions and provides global levels of abstraction is required. In our work, we take such an approach, particularly focusing on the receptor binding domain (RBD) of the SARS-COV2 spike protein with the human ACE2 receptor.

In the present article, we have investigated the three-dimensional structures of Human ACE2 receptor bound to SARS-CoV2 and SARS-CoV1, from a global non-covalent connectivity perspective, by explicitly considering the sidechain atomic details. We have analysed 10 μ s simulation trajectories (20) to characterise the interaction of the receptor binding domain (RBD) of the spike proteins with that of the ACE2 receptor. To this end, we construct a protein sidechain network (PSN) from the 3D protein complexes, as laid out in

Significance Statement

As the worldwide grip of the COVID-19 virus continues on in its ever-mutating forms, progress in combating it would benefit from alternate perspectives of its protein structure and the complex it forms with the human receptor. Here, we present a protein side-chain network characterization and percolation analysis of the complex, its connectivity, and its interface. We highlight the stronger interaction between COVID-19 and the human receptor in comparison to earlier coronaviruses. We show that the connectivity map hosts a wealth of information regarding mutations and the global structural changes brought about by local variations.

All the authors actively took part in the project. Specifically, MB, SmV and SaV designed the research, VS and AA generated data/plots/figures and contributed analytical tools. VS, AA, MB, SmV and SaV analysed data and performed research. VS, MB, SmV and SaV wrote the manuscript.

The authors are not aware of any competing interests.

(–) Current Affiliation

¹To whom correspondence should be addressed. E-mail: saraswathi@iisc.ac.in

previous works, with relevant details presented in the Methods section. In brief, the C_α atoms of each amino acid residue form the nodes of the PSN, and the edges between any two nodes signify the non-covalent interactions between them. The strength of interaction is estimated by considering all atoms of the two residues within a cutoff radius of 4.5 angstroms. The conventional non-covalent interactions such as disulphide bridges, hydrogen bonds, salt bridges, hydrophobic and stacking interactions are well defined and can be quantified in a pairwise manner. However, it is not straightforward to evaluate global connectivity using conventional methods. On the other hand, the metrics of the PSN - interface clusters, hubs, cliques and so on - offer crucial clues in understanding both the global connectivity of the network as well as local connectivity between key regions. It is also notable that such network metrics are dependent on edge interactions which are dynamic and fluctuate over time in equilibrium simulations(9). Our earlier works(21–25) extensively address this issue through graph spectral analysis alongside concepts borrowed from statistical physics. In particular, we demonstrate that these networks show percolation-like behaviour with respect to edge strength when the networks are dynamically averaged over the length of the simulation.

We apply these network methods to compare and contrast the global connectivity of both SARS-CoV1 and SARS-CoV2 bound to the human ACE2 receptor which form a protein complex. Our results show that globally, the largest cluster in the network is at the interface between the spike protein and ACE2 receptor in both cases, with the the SARS-CoV2 complex forming a more robust and dominant cluster in comparison to SARS-CoV1. At the atomic level, the interface cliques and communities reveal a more tightly held complex for SARS-CoV2. We also present analysis of certain specific snapshots chosen from the simulation trajectory to highlight fluctuations in time not captured by the dynamical averages, thus demonstrating the diversity of conformational landscapes explored during the course of the simulation. We also locate the mutated residues in key variants of concern/interest, which notably occur at the interface between the spike protein and the human receptor, further indicating its crucial role in global connectivity. Our analysis thus provides an atomistic map of the entire protein complex, based on optimal connectivity between spatially proximal amino acid residues. Such a map can act as a bridge to connect the local features with those observed or inferred from the global properties, thus providing a possible mechanistic explanation for the higher transmissibility/virulence of some variants over others. Therefore, our methods provide a basis to understand structure-function relationships and assess the outcome and design of drugs and antibodies in a rational manner.

Results and Analyses

As mentioned before, we construct the Protein Sidechain Network (See Methods section) such that the C_α atoms of each residue form the nodes of the network. The non-covalent interactions between any given pair of nodes labelled as i and j is captured by the edge strength parameter I_{ij} , expressed as a percentage. The nodes i and j are connected by an edge if their interaction strength I_{ij} is greater than a given threshold value, denoted as I_{min} henceforth. We perform our analysis over this constructed network at various threshold

values and lay out our key results in this section. We first present our results on the percolation-like behaviour of both complexes, dynamically averaged for varying values of I_{min} , with the predominant presence of interface residues in the largest cluster. We argue that the persistence of such a large interface cluster for higher threshold values in the SARS-CoV2 complex is an indicator of its higher robustness and dominance. These results also indicate the I_{min} values of significance in the network. We then focus on the nature of fluctuations in bond strength during the course of the simulation to further validate the indication of a robust interface. The dynamically averaged cliques and communities obtained at the interface form a connectivity map at the atomic level offering further evidence of a tightly held interface in the case of SARS-CoV2 as compared to SARS-CoV1. We finally discuss the network metrics of a few specific points in the simulation trajectory that highlight the diversity in the conformational landscape of individual snapshots of the complexes in comparison to the dynamical averages.

The Human ACE2 receptor complex forms a more dominant, robust cluster with the SARS-CoV2 spike protein as compared to SARS-CoV1.

We perform percolation analyses on the dynamically averaged spike protein-ACE2 receptor complexes of both SARS-CoV1 and SARS-CoV2, with results demonstrated in Figure 1. Crucially, it is seen that in both cases, the largest cluster formed in the network at lower I_{min} values(1 to ~2.75 %) is an interface cluster (IF-cluster, that is, one that contains nodes belonging to both the spike protein as well as the ACE2 receptor), encompassing most of the residues of both the proteins of the complex. However, the IF-cluster persists even at a higher stringency criteria of I_{min} ~3-4% mainly in the complex of SARS-CoV2 (Fig. 1(b)) as compared to SARS-CoV1 (Fig. 1(c)). Further, it is also seen that the IF-cluster continues to persist at higher I_{min} values of dynamic stability in the complex of SARS-CoV2 than in SARS-CoV1. The dynamic stability axis(details provided in the Methods section) gives us an indication of the statistical significance of the network's connectivity, as its conformations change through time in the MD simulations. Fig 1(a) highlights this aspect of the same data at two values (70% and 50%) of dynamic stability. At the 50% stability value, the more intricate nature of the interface percolation transition region in the complex of SARS-CoV2 is sharply contrasted against the near-sigmoidal nature of the SARS-CoV1 curve. In particular, the size of the largest IF-cluster falls steeply at I_{min} ~2.75 for SARS-CoV1, whereas SARS-CoV2 experiences an additional transition at I_{min} ~3.5. Further, the IF-cluster size is noticeably larger at I_{min} up to ~5.5. These observations strongly suggest the robust and dominant nature of interaction at the interface of the two proteins in SARS-CoV2-ACE2 complex.

Higher order connectivity and its visualization reveal tighter cliques and communities at the interface of the SARS-CoV2 complex as compared to the SARS-CoV1 complex.

The results in Fig. 1 yield a global, mesoscopic understanding of the interface interaction of the complexes. Motivated by this picture, we now investigate atomistic details of the network and present our results in Figures 2(a) and 2(b). Here we plot the dynamical average of the interaction strength of each edge against the standard deviation, which indicates the extent of fluctuation. The fluctuations of individual edges vary approximately in the

range of 1-6, in both the complexes, except for a few points reaching higher values in the case of SARS-CoV1 complex. Further, most of the fluctuating edges in SARS-CoV2 complex with average interaction strength (2-10) have standard deviation below the value of 4. The IF-edges are colour coded, based on average interaction strength and the interfacial edges with interaction strength greater than 2.3% are annotated with the interacting residue pairs. Consistent with the previous result, we see that a larger number of interfacial edges in the SARS-CoV2 complex (Figure 2(a)) have higher interaction strength (in the 2.3-3.8% region) as compared with the SARS-CoV1 complex (Figure 2(b)). We also present a panel in Figure 2(c) that shows sequence alignment of the amino acid residues of the two spike proteins that participate in the interface bonds, thus mapping certain interfacial edges onto each other. The details of the edges displayed and their strengths are compared in Table 1 in the Supplementary Material.

Interestingly, many of the fluctuating edges at the interface are also part of IF-cliques/communities. Additionally, edges in both complexes with average interaction strength beyond 10 form interface cliques and communities, while also possessing higher fluctuations in edge strengths. They are likely to play an important functional role by exploring a wider conformational space. Thus, it is useful to also compare the two complexes at the next level of higher order connectivity (IF-cliques/communities), and the corresponding spike - receptor binding domain (RBD) residues. The interface cliques of both complexes associated with the averaged network at $I_{min} = 2.75$ are shown in Figure 3(a,b). The Figures 2(d) and 2(e), highlight the locations of the interfacial edges on the 3D representations of the two protein complexes (shown on Pymol of the reference structure). The average IF-edges (the colour coded strength as in Figure 2(a-b)), presented here indicates the stronger nature of interface interaction between the spike protein and the receptor protein for SARS-CoV2, in terms of the cliques/communities they form. It also underscores the position of functionally important residues like Lys417, Asn501, Leu455, Tyr505 at the community level, many of them are found to be mutated in the variants of interest (VOI).

We focus on a few noteworthy features highlighted by the results on interface edges and their corresponding cliques structure presented so far. The interactions of certain aligned spike protein residues like Val404/Lys417, Tyr442/Leu455, Pro464/Ala475, Leu472/Phe486, and Tyr484/Gln498 (See Figure 2(c)) with the residues of the ACE2 receptor are important to our analysis here. We also draw attention to the edges formed by methionine 82 and tyrosine 83 (ACE2 receptor) with phenylalanine 486 (SARS-CoV2) and lysine 417 (SARS-CoV2) with residues aspartic acid 30 and histidine 34 (ACE2 receptor). The loop held by the disulphide bridge in the two spike proteins [SARS-CoV2 (Cys480-Cys488) and SARS-CoV1(Cys467-Cys474)], and their amino acid compositions [CoV2-CNGVEGFNC- versus CoV1-CTPPALNC], has played a crucial role in their interaction with the ACE2 receptor. This loop in SARS-CoV2 is not only longer by one residue, but also contains two flexible glycine residues, in contrast with two highly rigid proline residues in SARS-CoV1. This has enabled SARS-CoV2 to comfortably latch on to the residues methionine 82 and tyrosine 83 of the ACE2 receptor. Furthermore, the interaction between the loop (Cys480-Cys488) is retained even at higher interaction strength of $I_{min}=4.5$. Such

differences have led to subtle rearrangement of IF-interactions and their average strengths, leading to significant differences in their connectivities.

More explicitly, the accessible amino acid residues of the ACE2 receptor are tightly captured by the RBD region of SARS-CoV2 amino acid residues. Although the RBD residues of SARS-CoV1 are exposed to the same residues of the ACE2 receptor, it is unable to bind strongly with the residues like Met82, Tyr83 on one face of the complex and to the residues Glu37 and Arg 393 on the opposite face. Further, the residue Lys417 of SARS-CoV2 also plays a significant role by reaching out a long helical stretch (from Asp30 to His34) of the accessible face of the ACE2 receptor, as well as making a strong network of cliques. Such an active connectivity-role is unmatched by the corresponding residue Val404 of SARS-CoV1. Figure 2(a-e) and Table1 provide various parameters to support this fact and finally, the explicit atomic details of the interface sidechains are depicted by the pymol representation of the two complexes in Figure 2(d,e).

Higher affinity of SARS-CoV2 to ACE2 receptor as compared to SARS-CoV1 is associated with a higher interaction strength of the IF-cluster.

For a given network, a cluster represents more global connectivity than the metrics like edges, hubs, and cliques. As seen in Figures 4(a,b), the largest interface cluster at $I_{min} \leq 2.75$ is dominated by the ACE2 receptor in both the complexes. This situation remains unaltered for higher I_{min} values in the cases of SARS-CoV1 complex, whereas a major part of ACE2 receptor separates from the interface cluster around $I_{min} \sim 3.2-3.5$ in the case of SARS-CoV2 complex. Further, despite the ACE2 receptor dominating the interface cluster for both complexes at weaker I_{min} , we observe clear distinctions between the two cases, in terms of the continuity of the connections at interface. A careful analysis of the corresponding building blocks, cliques/communities in Figure 3(a, b) also exhibit differences. Specifically, these units are well interspersed between the residues of SARS-CoV2 and ACE2 receptor, whereas two out of the three communities in SARS-CoV1 and ACE2 receptor complex are highly biased towards the spike protein residues. The continuity of the interface connections in the SARS-CoV2-ACE2 receptor complex arises due to the interface communities, which are robust ($I_{min} \geq 3.5$) and they are stitched beautifully well with strong edges. Furthermore, the robustness leads to a strong interface cluster, which separates itself from a major part of the ACE2 receptor.

We also present a conventional 3D-pictorial representation (Pymol) of both complexes for various I_{min} in Figures 5 and 6. This feature is consistent with the largest cluster transition profiles as function of I_{min} at 50% dynamic stability as seen in Figure 1(a). The stability of the largest interface cluster at higher interaction strengths in SARS-CoV2 complex as compared to SARS-CoV1 complex indicates that information regarding higher binding affinity can be extracted from the size of the largest interface cluster. To the best of our knowledge, we have not encountered any studies in literature relating the binding affinity between protein-protein interactions being connected to the interface cluster, with strong non-covalent interactions. This analysis shows that the interface network parameters from the simulation averages indicate a stronger affinity of ACE2 receptor with SARS-CoV2 than with SARS-CoV1. However, the metrics from simulation averages is indeed a good reflection of the conformations of the individual

snapshots, obtained from simulations in both the complexes.

To summarize, the PSN-network metrics of the simulation averages suggests stronger binding of the SARS-CoV2 than SARS-CoV1, with the ACE2 receptor. This feature is clearly seen in individual snapshots of the SARS-CoV2 complex as well. In the next section, we provide network analysis of a few selected individual snapshots of the SARS-CoV2 complex, to understand the level of structural diversity in the conformational landscape.

Comparing individual conformations shows that while cliques and communities are stable in SARS-CoV2, there exist prominent variations involving key functional residues.

We now focus on presenting a few selected conformations of the complex at higher I_{min} values. Since the SARS-CoV1 complex has already undergone the percolation transition at these I_{min} values and the size of the IF cluster is no longer significant, we mainly present the details of interface clusters in snapshots of the SARS-CoV2 complex. We selected the structures (a) Reference, (b) High RMSD, and (c) End, for our analysis, which correspond respectively to the initial equilibrated structure, the snapshot with high RMSD with the Reference, and a snapshot towards the end of the simulations. Comparing individual conformations shows that while cliques and communities are stable, variations involving key functional residues are prominent. This is evident from the results presented here. The IF-cliques and communities (at $I_{min} \geq 3.5$) in the three selected snapshots of SARS-CoV2 complex are consolidated in Figure 7 (a, b, c). It highlights two major points: (a) The amino acid residues in the cliques and communities are mutated (except for Leu 455, until the appearance of currently circulating recombinant variant of interest JN.1), giving rise to variants and secondly, (b) although the cliques are very much similar, they are not identical, clearly showing the diversity of structures at the network level, in the conformational landscape explored during the simulations. That is, a continuous network across the interface in the SARS-CoV2 complex is achieved through robust cliques and communities in the selected snapshots. The network diversity between the three selected structures becomes even more striking with distinctly different conformational states at the IF-cluster level as shown in Figure 8 (a, b, c). Below we highlight a few points from this perspective.

In the previous section we highlighted the important role of the loop (Cys480-Cys488) in the context of the average behaviour of the SARS-CoV2-ACE2 Receptor complex. This nine-residue loop consisting of the sequence -CNGVEGFNC-, is loaded with structurally influential amino acids. First, it is long enough to latch on to helix 1 of the ACE2 Receptor and also is able to interact with residues like Met82, Tyr83. The two glycine residues (482 and 485) of the loop allow high flexibility, thus accommodating various conformations required at different functional states. For example, one of the cliques of the End structure (Figure 7c) is made up of N481 and F486 with M82 of the Receptor protein.

A majority of RBD residues of SARS-CoV2 interact with the first 2 helices (ranging from Gln24 to Tyr41) and a few other residues (e.g., N330, K353, R357, R393) of the ACE2 Receptor. They act as player nodes of the two parties. The collection of cliques and communities from the three selected structures in Figure 7 (a, b, c) clearly demonstrates the subtle structural diversity brought out by the same set of nodes by

regrouping differently. A collection of them and rearrangements with respect to the interface region of the complex is shown in Figure 9.

The integration of the cliques and communities in the interface clusters brings another dimension of diversity as shown in Figure 8 (a, b, c). The diversity in the interface cluster is brought out by connecting different combinations of cliques/communities. The Reference structure (Figure 8a) has two arms, connected by a hinge region, interestingly is held by the largest community. The IF-cluster regions of the arms are supported mainly by the ACE2-Receptor residues, whereas the hinge region is supported by the RBD residues of SARS-CoV2. By and large, most of the mutations have occurred in IF-cluster. It is noteworthy that until recently the residue L455 was not reported, although it occupies a prominent position in the community and connected to influential residues like K417, Q498. Perhaps it acts as a buffer to maintain the community during dynamical processes. More about this residue will be presented in the Discussion section. The IF-cluster in high RMSD structure (Figure 8b) has split up into two clusters. The largest community here is made up of residues such as F498, N501, Y505 of SARS-CoV2, which are connected to mainly the ACE2 Receptor. The second part of the interface cluster is not dense with communities. However, it has retained the four-residue community with K417 and L455 and a linear connectivity with helix 1 and the residue M82 of the ACE2 Receptor, with the residues of the loop Cys480-Cys488 of SARS-CoV2. Thus, the high-RMSD structure has adopted a strategy of splitting the IF-cluster into two parts, with one of them latching on the Cys480-Cys488 loop and the other, exploring the residues closer to the cleavage site. Finally, the End structure (Figure 8c) offers a glimpse of a large IF-cluster, connecting the entire length consisting the loop latching to M82, passing through the hinge region (K417, L455, Q493) and reaching the activity centre, consisting of important functional residues.

To summarize, the robustness of the interaction between the ACE2 Receptor and the RBD region of the SARS-CoV2 at higher interaction strength is evident from the network metrics of interface cliques/communities, and the interface clusters. More importantly, the conformational diversity depicted by subtle reorganization of the same set of amino acids from the viral protein and the host -ACE2 Receptor is highly impressive.

The importance of network parameters in rationalizing some of the mutations and the relevance of conformations diversity at network level, will further be dealt with in the Discussion section.

Discussion. In the Results section we have presented a rigorous analysis of the simulation trajectories of the complexes that the human ACE2 receptor forms with the COVID-19 virus SARS-CoV2 and the earlier coronavirus SARS-CoV1 (20). The analyses, with focus on the interfaces of the viral protein and the ACE2 receptor protein, have provided global connectivity maps, based on the complex structure-networks of non-covalent interactions. Network metrics such as edges, cliques, and clusters have provided a wealth of local details in the context of global connectivity. In other words, the connectivity from the one-dimensional edge level interaction leading to three-dimensional higher order topological units, culminating in globally connected clusters are systematically tracked through detailed connectivity maps. Furthermore,

the dependence of global connectivity on edge weights has unraveled intricate changes that undergo in the dynamical state. The percolation behavior, observed for the simulation averages has clearly shown that at higher interaction strength, the SARS-CoV2 complex is more stable than the SARS-CoV1 complex. The specific interactions and their fluctuations are captured at the edge level and their tracking through higher order connectivity metrics has clearly exhibited the dynamically stable behavior of SARS-CoV2 complex than SARS-CoV1 complex. Apart from the average behavior, the analysis of individual snapshots of the SARS-CoV2 complex has provided a landscape of conformations, with subtle differences in their cliques, communities, and the IF-clusters, which are not captured by conventional parameters such as root mean square deviation (RMSD) of the overall backbone structure. Needless to mention that such a connectivity map can be useful in many ways, such as locating the position and the topological status of relevant residues of the viral protein as well as the interacting residues of the ACE2 receptor in the global context. For example, such a map can assist in placing the mutations of variants on the global map or in designing drugs and vaccines.

In our concluding analyses below, we underscore the importance of the connectivity map and the network topological metrics, which would have been difficult to rationalize through direct interface connections alone. We specifically discuss: (A) Locating the SARS-CoV2 mutations on the sidechain non-covalent connectivity map and to understand the effects of mutations on affinity towards ACE2 receptor and related functions, (B) to understand the rationale behind the efficacy of designed ACE2 decoy receptors to effectively neutralize the Coronaviruses, which are constantly evolving.

The 3D-map generated from the PScN complex allows pinpointing of mutations. A major fraction of mutations in the receptor binding domain (RBD) of SARS-CoV2 have occurred at the interface clusters of the complex with ACE2 receptor. Since the emergence of the COVID-19 pandemic at the end of 2019, extensive sequencing of SARS-CoV2 has been carried out. We refer the reader to Table 2 of Reference (26) containing the WHO classification of variants along with the other amino acid substitutions observed represented among the 303,250 human SARS-CoV2 spike protein sequences. Interestingly, the mutations in RBD of the spike protein are minimal, compared to the entire viral genome. However, the crucial first step of attack is the binding of RBD with the ACE2 receptor. A significant number of structures of the complex with ACE2 receptor has also become available from X-ray and cryo EM studies. As expected, most mutations are at the binding site. Although the direct interactions between the residues of SARS-CoV2 and ACE2 receptor are obvious from the structures, there are several of them which can be detected only through the network representation.

Here we highlight some of the mutated residues reported in literature, on our connectivity map of the IF-Cluster, generated at the edge interaction strength $I_{ij} \geq 3.5$ in Figures 10 and 11.

The genome of the virus SARS-CoV2 has several subdomains among which, the Spike protein is considered as the most important domain to enter the host cell through the ACE2 Receptor. The number of mutations in this protein is about 4000. However the Receptor Binding Domain (RBD) of this protein has only a few mutations (27–29) New active

variants are still emerging and one needs to understand the complete mechanism of various aspects such as intensity of infection, escape mutations, rate of transmissibility and so on.

An extensive diversification of Omicron sublineages has taken place in the past two years (28). Among them, the subvariants BQ.1 and XBB.1 are reported to be the most resistant SARS-CoV2 variants. Recombination of various sublineages spreading simultaneously, have led to complex-recombinant lineages, making it difficult to track the lineage of off-springs through conventional approaches. Extensive experimental studies and analyses are being conducted to address the problem of induced convergent evolution of Omicron-RBD domain(29, 30). Figure 12 (borrowed and presented as is from Reference (29)) provides a lucid picture of evolutionarily conserved mutations in the emergent variants. In addition, other variants of SARS-COV-2 BA.2.86 lineage (31) such as JN.1(L455S mutation), and Flip Variant with mutations (L455F; F456L) are currently posing challenges with high transmissibility/binding affinity, in several parts of the globe. With this background of constantly evolving variants of concern/interest, we provide a perspective from the structure network of SARS-CoV2 complex with ACE2 receptor in the following paragraph. We make use of the network topological metrics such as cliques, communities, and the clusters at the host-pathogen interface, described in the Result section to explore if the mutations have any correlation with their topological metrics.

Figures 7, 8, and 9 clearly indicate that most of the mutations are embedded in cliques/communities, which are generally parts of the largest IF-Clusters. Here we compare a few of these residues with the set of mutated residues presented on the Y-axis of Figure 12, which are implicated to be involved in convergent evolution of Sars-CoV2-RBD region. For example, R493 of BA.5 variant has reverted back to the original Wuhan strain Q493 and interestingly, in two simulation snapshots (7a, 7b), it occupies a prominent position in the community. Similarly, Q498 also occupies a prominent position in the community (including the key residue N501) in all the three snapshots (7a-c). Although Q498 is not listed in Figure 12, it is attached to G447 in the IF-cluster (8a) and its sequential neighbours G446 and V445 that are listed in Figure 12, have possibly undergone convergent evolution to serine and proline residues respectively, which can greatly influence the conformational landscape.

Finally, the JN.1 and the Flip Variant with mutations (L455F; F456L) are interesting cases to view from structure network perspective. Until recently, mutations in L455 were not observed. Looking at its crucial position in the community containing K417 and several other key residues, we were intrigued by its resistance to mutation. Now, in JN.1 it is mutated to a small serine residue. The flip variant is even more interesting, by swapping the leucine residue with the obligatory sequence neighbour F456, essentially maintaining the leucine environment in the vicinity. Thus, the connectivity map can provide a wealth of information in understanding complicated mechanisms such as allostery, paths of communication, evolution of sequence-function relationships (11) or inferring the effect of mutations from a global structural perspective.

The global connectivity map can potentially assist in designing ACE2 decoy receptors to neutralize the Coronaviruses. As a treatment towards SARS-CoV2 infection, monoclonal

antibodies(mAbs) and their cocktail forms are designed to combat viral evasion. However, the evolution of Omicron and other variants of SARS-CoV2, such as BQ.1, XBB have managed to evade neutralization due to their escape mutations. Thus, the concept of engineered ACE2 decoy receptors has been explored to neutralize SARS-CoV2 virus evasion and the clinical studies have gained momentum in recent times.

Various experimental and computational strategies (32–34) are used for the design procedure. One of the concepts is to identify the amino acid residues of the human ACE2 receptor, involved in binding (directly or indirectly) to receptor binding domain (RBD) of SARS-CoV2 spike protein and design the ACE2 receptor residues for better binding. In this context, we believe that our map can assist in predicting the viable residues, specifically those which make indirect contact that are difficult to identify by conventional methods. To be precise, we can investigate the residues which contribute to better binding through cliques, communities, and part of strong interface cluster (IF-Cluster). As an example, we examine the ACE2 receptor residues which have shown enhanced affinity upon mutation in Reference (35). In this study the authors have identified several residues as shown in Figure 13.

We take the example of the IF-cluster of the Reference structure to map the mutations in the ACE2-Receptor as seen in Figure 13. The orange circles in Figure 10 encompass the ACE2-Receptor mutations. We notice a few interesting correlations of the affinity enhancement in ACE2 receptor with our global map. Specifically, the important residues of the first 2 helices of the ACE2 receptor have shown preference to aromatic/planar/ sidechains[T27(W,Y,F,K); K31(N,M,F,W); E35(K,Q) as seen in Figure 11. The residue T27 of the ACE2 receptor in this interface cluster is sandwiched between two aromatic residues (F456 and F489) of SARS-CoV2 -RBD, whose stability is strongly enhanced by the replacement of T27 by aromatic residues. In fact, F456 and F489 are connected on their other sides by aromatic residues Y473 of SARS-CoV2 and F28 of ACE2 receptor respectively. In addition, F28 is part of a community of two 3 residue cliques of ACE2 receptor which are largely made up of aromatic residues [F32, F72, Q76]. The aliphatic residue L79 has shown enhancement of affinity by F and T replacements. Thus, in principle, the engineered ACE2 receptor can have a stretch of aromatic residues strongly connecting the middle segment of the interface region, with K417 of SARSCoV2 to the end region with M82-Y83 of ACE2. Furthermore, the mutation M82 to Y will further strengthen the aromatic connection of this stretch and the mutation of A25 to V will increase the hydrophobic interactions with the neighbouring residues. In the same region, the residue Q101 is shown to prefer H, which is buried in the crystal structure [PDB: 6m0j](36). However, it is possible to change its exposure status, since it is close to the beginning region (Y83-M82) of the interface, as seen from our interface cluster map. The interface clique/community consisting of (R357 and N330 of the Ace2 receptor with T500 of SARS-CoV2), is present in all the three structures which we have chosen for the analyses (Figure 9). Additionally, they are also part of IF clusters in which R357, W48, and W349 of ACE2 receptor are connected to each other. Thus, the substitution of N330 by aromatic residues (F,Y) can make a strong aromatic connection to T500 of SARS-CoV2, which has a functional role near the cleavage site. Thus, the designed mutations in the ACE2-Receptor are

contributing to higher stability of the interface cluster or alter the conformation to be exposed or buried within the complex.

Conclusion

In summary, the network representation of all non-covalent interactions in the protein structures of the complexes that the human ACE2 receptor forms with the COVID-19 virus SARS-CoV2 and the earlier coronavirus SARS-CoV1 performed here, provides a three-dimensional map, which can be quantified in terms of network metrics such as cliques, communities and clusters. In other words, the connectivity from the one-dimensional edge level interaction leading to three-dimensional higher order topological units, culminating in globally connected clusters are systematically tracked through detailed connectivity maps. Here we have specifically captured the interface interactions, their strengths and fluctuations at the edge level, and their contributions to the global connectivity and the percolation behaviour, observed for the simulation averages, tracking through higher order topological metrics. These network based analyses have clearly exhibited the dynamically stable behaviour of SARS-CoV2 complex than the SARS-CoV1 complex, which cannot be captured by conventional structure analysis parameters like RMSD.

Based on our analyses of individual snapshots, we find that while the amino acid residues participating at the interface edges, cliques, and communities of SARS-CoV2 and the ACE2 receptors, are by and large common as seen from the simulation averages, the diversity is brought out at the interface cluster level. Thus, we underscore the subtle reorganization of the connectivity of different units leading to diversity in the conformational landscape, in which the conformations can dynamically switch from one to another, facilitating specific functions.

We have demonstrated the utility of the connectivity map in pinpointing the position and the topological status of residues involved in mutation/evolution of the viral protein as well as the ACE2 receptor residues, which aid in designing decoy ACE2 receptors for combating viral attack.

In conclusion, the network approach presented here to characterize Covid-19- Human ACE2 receptor can be adopted to understand the mechanism of host-pathogen interaction in general, since the connectivity map can provide a wealth of information in understanding complicated mechanisms such as allostery, paths of communication, evolution of sequence-function relationships and so on. A better understanding of fundamental principles is required to gain insights to the folding process of proteins in the cell environment (37). Parallely, the AI based AlphaFold (38) can model protein structures from sequences with high accuracy and unimaginable speed. With all the current advances, an exciting future can be expected in the understanding of the role and control of proteins in the functioning of cells.

Methods

Dataset: The data for 10 μ s molecular dynamics simulation trajectories of the human ACE2 receptor in complex with the receptor binding domains of the spike protein of the SARS-CoV1 coronavirus (PDB: 2AJF) as well as the SARS-Cov2 coronavirus (PDB: 6M17) were obtained from DE Shaw Research (20). The SARS-CoV1 complex has 777 amino acid

residues while the SARS-CoV2 complex has 775 residues. This data was further processed to extract 99 snapshots from the trajectories sampled at equal intervals of time for each complex. These two sets of 99 snapshots each form the basis of our analysis, and the input to PSN-Ensemble.

Construction of Protein Structure Networks and their dynamics: We have performed the sidechain non-covalent connectivity network analyses on the structures of the complexes of SARS-CoV1 and SARS-CoV2(COVID-19) spike proteins with Human ACE2 receptor. The network analyses are performed on (i) the average connectivity matrix from the simulation snapshots and (ii) on selected snapshots which show commonality and differences in their network parameters such as cliques, communities and large clusters, with focus on the interface region between the ACE2 receptor and the RBD of the spike proteins. Focusing first on the average connectivity matrix, it is obtained based on two inputs - the threshold edge interaction in each network snapshot and the threshold statistical significance of each edge interaction over all the snapshots. A brief summary of the evaluation of the average network based on these parameters is provided below. The detailed methodology is provided in earlier papers/reviews (21–25).

Each snapshot is translated to a network where the non-covalent connectivity within a protein structure as well as across the complex are considered as edges, and the nodes can be either the backbone atoms such as C- α atom or an amino acid residue(including all atoms of the sidechain) of the polypeptide chain. Here we have considered the protein sidechain network (PScN), to capture the subtleties of sidechain conformations through weighted edges as given in the equation 1 (25, 39). The interaction between two nodes i and j is given by

$$I_{ij} = \frac{n_{ij}}{\sqrt{N_i N_j}} \times 100 \quad [1]$$

where n_{ij} is the number of atom pairs between two given residues i and j , within a distance cutoff of 4.5 angstroms, and N_i/N_j are normalization values defined as the maximum possible number of contacts that the residues i and j can make across a nonredundant database. A weighted PScN is constructed by comparing I_{ij} to the user-defined threshold I_{min} to obtain a binary matrix of connectivity.

The average network as defined over all such snapshots requires the second user-defined parameter that we call dynamic stability. Consider the elementary example in Fig. 14. Fig. 14(a) shows a collection of networks obtained from snapshots across a simulation trajectory where each edge has a weight of 1. Fig. 14(b) is a matrix showing the percentage of the total snapshots in which each edge appears. Thus, it is a matrix of statistical significance of the particular edge across the snapshots. Dynamical stability thus specifies the threshold for this value of statistical significance for each edge in the average network. The average networks for three such dynamical stability values are shown in Fig. 14(c).

Percolation Transition Profile: Based on the atomic connectivity metrics I_{ij} given in Eq 1, the threshold I_{min} is expressed as a percentage. For protein structures, it is shown that the profile of I_{min} versus the size of the largest cluster thus obtained exhibits a sigmoidal curve, analogous to the percolation

phenomenon (40, 41). That is, for a fixed value of dynamic stability and low values of I_{min} , the network is dense, leading to a maximally connected cluster that spans system size by upto 80-90%. For higher values of the threshold, the largest cluster size consists only of the very strongly connected edges, which do not span system size. The resulting value of I_{min} with a steep transition in size of the largest cluster is called the percolation point. This point aids us in selecting a normalized connectivity value, which is an optimal nucleation point. The addition of edges with connectivity lower than the transition point will enhance the size of the largest cluster, while setting I_{min} higher than the value at the transition point, yields stronger localized clusters (21). Although such a profile is seen largely in globular protein structures, factors such as the interaction of protein-protein complexes can influence the details of the transition profile. In the current study we have observed such changes and have found it to be relevant to distinguish SARS-CoV1 and SARS-CoV2 binding with ACE2 receptor, which have been elucidated in the Results section.

The clusters, cliques and communities can also be evaluated for individual snapshots without the application of any averaging technique. We perform these analyses for selected snapshots to highlight the effects of connectivity in the complexes.

Visualisation: All our data is primarily visualized using PY-MOL and Cytoscape, with some figures being generated on Adobe Illustrator.

Data Sharing: Data and codes are available upon reasonable request to the authors.

ACKNOWLEDGMENTS. SaV would like to acknowledge the NASI Honorary Scientist Fellowship.

1. D Mannar, et al., Sars-cov-2 omicron variant: Antibody evasion and cryo-em structure of spike protein-ace2 complex. *Science* **375**, 760–764 (2022).
2. PH Guzzi, et al., Computational analysis of the sequence-structure relation in sars-cov-2 spike protein using protein contact networks. *Sci. Reports* **13**, 2837 (2023).
3. A Zabiegala, Y Kim, KO Chang, Roles of host proteases in the entry of sars-cov-2. *Animal Dis.* **3**, 12 (2023).
4. DA Jamison, et al., A comprehensive sars-cov-2 and covid-19 review, part 1: Intracellular overdrive for sars-cov-2 infection. *Eur. J. Hum. Genet.* **30**, 889–898 (2022).
5. SA Narayanan, et al., A comprehensive sars-cov-2 and covid-19 review, part 2: host extracellular to systemic effects of sars-cov-2 infection. *Eur. J. Hum. Genet.* **32**, 10–20 (2024).
6. N Maroli, Riding the wave: Unveiling the conformational waves from rbd of sars-cov-2 spike protein to ace2. *The J. Phys. Chem. B* **127**, 8525–8536 (2023).
7. BT Kaynak, et al., Sampling of protein conformational space using hybrid simulations: A critical assessment of recent methods. *Front. Mol. Biosci.* **9** (2022).
8. B Wingert, J Krieger, H Li, I Bahar, Adaptability and specificity: how do proteins balance opposing needs to achieve function? *Curr Opin Struct Biol* **67**, 25–32 (2020).
9. D Scaramozzino, RL Jernigan, Special issue on computational approaches for protein dynamics and function. *Appl. Sci.* **13** (2023).
10. B Jawad, P Adhikari, R Podgornik, WY Ching, Key interacting residues between rbd of sars-cov-2 and ace2 receptor: Combination of molecular dynamics simulation and density functional calculation. *J. Chem. Inf. Model.* **61**, 4425–4441 (2021).
11. AS Pillai, GK Hochberg, JW Thornton, Simple mechanisms for the evolution of protein complexity. *Protein Sci.* **31**, e4449 (2022).
12. A Ali, R Vijayan, Dynamics of the ace2-sars-cov-2/sars-cov spike protein interface reveal unique mechanisms. *Sci. Reports* **10**, 14214 (2020).
13. C Bai, A Warshel, Critical differences between the binding features of the spike proteins of sars-cov-2 and sars-cov. *The J. Phys. Chem. B* **124**, 5907–5912 (2020).
14. Y Cai, et al., Distinct conformational states of sars-cov-2 spike protein. *Science* **369**, 1586–1592 (2020).
15. C Xu, et al., Conformational dynamics of sars-cov-2 trimeric spike glycoprotein in complex with receptor ace2 revealed by cryo-em. *Sci. Adv.* **7**, eabe5575 (2021).
16. M Noval Rivas, RA Porritt, MH Cheng, I Bahar, M Arditi, Multisystem inflammatory syndrome in children and long covid: The sars-cov-2 viral superantigen hypothesis. *Front. Immunol.* **13** (2022).
17. G Verkhivker, S Agajanian, R Kassab, K Krishnan, Computer simulations and network-based profiling of binding and allosteric interactions of sars-cov-2 spike variant complexes and the host receptor: Dissecting the mechanistic effects of the delta and omicron mutations. *Int. J. Mol. Sci.* **23** (2022).

18. R Nussinov, M Zhang, Y Liu, H Jang. Alphafold, artificial intelligence (ai), and allostery. *The J. Phys. Chem. B* **126**, 6372–6383 (2022).
19. JPA Ioannidis, F Zonta, M Levitt, Variability in excess deaths across countries with different vulnerability during 2020–2023. *Proc. Natl. Acad. Sci.* **120**, e2309557120 (2023).
20. DES Research, Molecular dynamics simulations related to sars-cov-2 (2020) D. E. Shaw Research Technical Data, https://www.deshawresearch.com/downloads/download_trajectory_sarscov2.cgi/.
21. A Halder, et al., Surveying the side-chain network approach to protein structure and dynamics: The sars-cov-2 spike protein as an illustrative case. *Front. Mol. Biosci.* **7** (2020).
22. V Gadiyaram, S Vishveshwara, S Vishveshwara, From quantum chemistry to networks in biology: A graph spectral approach to protein structure analyses. *J. Chem. Inf. Model.* **59**, 1715–1727 (2019) PMID: 30912941.
23. M Bhattacharyya, S Ghosh, S Vishveshwara, Protein structure and function: Looking through the network of Side-Chain interactions. *Curr Protein Pept Sci* **17**, 4–25 (2016).
24. M Bhattacharyya, CR Bhat, S Vishveshwara, An automated approach to network features of protein structure ensembles. *Protein Sci.* **22**, 1399–1416 (2013).
25. N Kannan, S Vishveshwara, Identification of side-chain clusters in protein structures by a graph spectral method¹ edited by j. m. thornton. *J. Mol. Biol.* **292**, 441–464 (1999).
26. K Guruprasad, Mutations in human sars-cov-2 spike proteins, potential drug binding and epitope sites for covid-19 therapeutics development. *Curr. Res. Struct. Biol.* **4**, 41–50 (2022).
27. B Cosar, et al., Sars-cov-2 mutations and their viral variants. *Cytokine & Growth Factor Rev.* **63**, 10–22 (2022).
28. C Roemer, et al., Sars-cov-2 evolution, post-omicron (2022) <https://virological.org/t/sars-cov-2-evolution-post-omicron/911>.
29. Y Cao, et al., Imprinted sars-cov-2 humoral immunity induces convergent omicron rbd evolution. *Nature* **614**, 521–529 (2023).
30. JD Bloom, RA Neher, Fitness effects of mutations to sars-cov-2 proteins. *Virus Evol.* **9**, vead055 (2023).
31. Y Kaku, et al., Virological characteristics of the sars-cov-2 jn.1 variant. *bioRxiv* (2023).
32. MC Chan, KK Chan, E Procko, D Shukla, Machine learning guided design of high-affinity ace2 decoys for sars-cov-2 neutralization. *The J. Phys. Chem. B* **127**, 1995–2001 (2023).
33. Y Huang, C Yang, Xi Xu, W Xu, Sw Liu, Structural and functional properties of sars-cov-2 spike protein: potential antiviral drug development for covid-19. *Acta Pharmacol. Sinica* **41**, 1141–1149 (2020).
34. C Chen, et al., Computational prediction of the effect of amino acid changes on the binding affinity between sars-cov-2 spike rbd and human ace2. *Proc. Natl. Acad. Sci.* **118**, e2106480118 (2021).
35. T Arimori, et al., Engineering ace2 decoy receptors to combat viral escapability. *Trends Pharmacol Sci* **43**, 838–851 (2022).
36. J Lan, et al., Structure of the sars-cov-2 spike receptor-binding domain bound to the ace2 receptor. *Nature* **581**, 215–220 (2020).
37. SJ Chen, et al., Protein folds vs. protein folding: Differing questions, different challenges. *Proc. Natl. Acad. Sci.* **120**, e2214423119 (2023).
38. J Jumper, et al., Highly accurate protein structure prediction with alphafold. *Nature* **596**, 583–589 (2021).
39. R Sathyapriya, MS Vijayabaskar, S Vishveshwara, Insights into protein–dna interactions through structure network analysis. *PLoS Comput. Biol.* **4**, 1–15 (2008).
40. K Brinda, S Vishveshwara, S Vishveshwara, Random network behaviour of protein structures. *Mol. BioSystems* **6**, 391–398 (2010) Copyright: Copyright 2010 Elsevier B.V., All rights reserved.
41. D Deb, S Vishveshwara, S Vishveshwara, Understanding protein structure from a percolation perspective. *Biophys. Journal* **97**, 1787–1794 (2009).

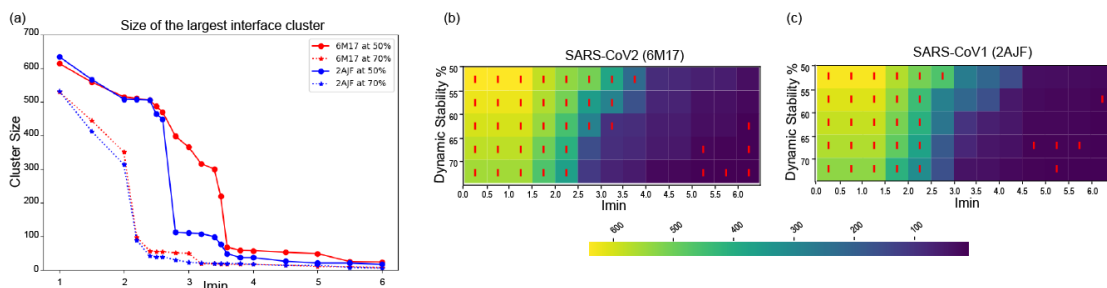


Fig. 1. Mesoscopic view of global connectivity maps of spike protein – ACE2 receptor complexes reveal stronger percolation behavior in SARS-CoV2 compared to SARS-CoV1 : (a-c) Percolation analyses of the largest cluster, particularly those at the interface (highlighted as I in red) have revealed a tighter interface. We see retention of interface clusters at the higher stringency criteria of I_{min} 3-4% and higher dynamic stability cut-offs in SARS-CoV2 as compared to SARS-CoV1. Here, we focus on MD simulation trajectories. The differences between the two complexes are clearly seen to be more apparent at dynamic stability 50% than at higher values. In Fig (a), the data at 50% and 70% are highlighted to demonstrate these differences. In particular, it is seen that at 50% dynamic stability, it is seen that the size of the largest interface cluster only falls at I_{min} value ~ 3.5 for SARS-CoV2 as opposed to I_{min} of ~ 2.75 for SARS-CoV1. The variation of the curve for intermediate values of dynamic stability are shown in Figures (b) and (c) for SARS-CoV2 and SARS-CoV1 respectively.

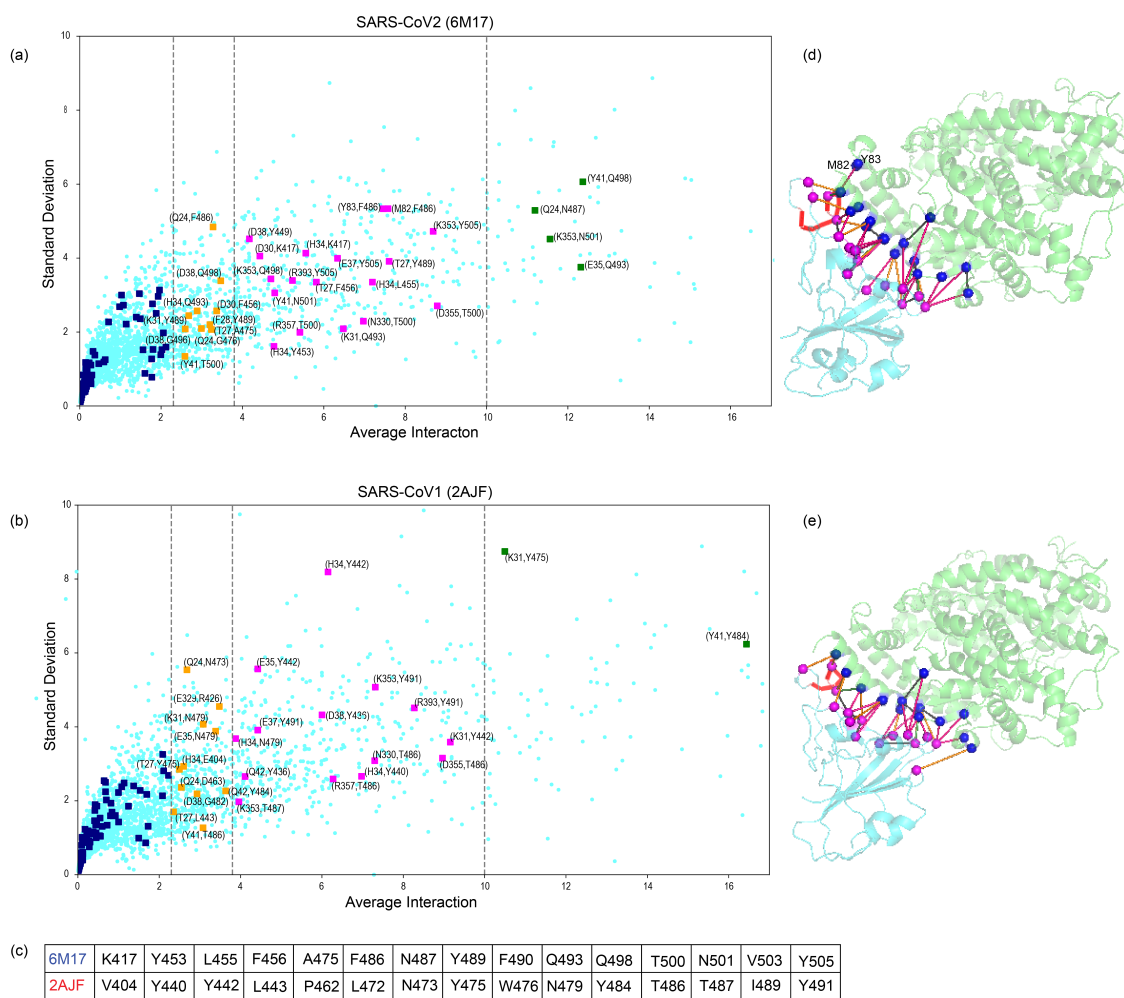


Fig. 2. (a,b) Atomistic details of the stronger interface in 6M17 versus 2AJF. This is a zoomed-in view of all edge interaction strengths in the spike-ACE2 complex structure network across the conformational ensemble obtained from the MD simulations. We plot the edge interaction strengths for all pair of residues averaged over all the MD trajectory snapshots against the standard deviation in the interaction strengths. This value signifies the fluctuations from the average edge strength for the corresponding pair. We have also highlighted the interface residue pairs (I,J) where I comes from the ACE2 receptor and J from the spike protein. The vertical grey lines divide the plots to bin the interface edges in four intervals based on average interaction. These intervals are color-coded as navy (0-2.3), orange (2.3-3.8), magenta (3.8-10) and green (over 10). (c) The table below maps the 6M17 spike protein residues to structurally equivalent residues in 2AJF. (d,e) Pymol representations of protein complexes are also shown alongside, highlighting the interface edges. The loop held by the disulphide bridge in the two spike proteins [SARS-CoV2 (Cys480-Cys488) and SARS-CoV1 (Cys467-Cys474)] are marked as a red ribbon in each of the protein complexes

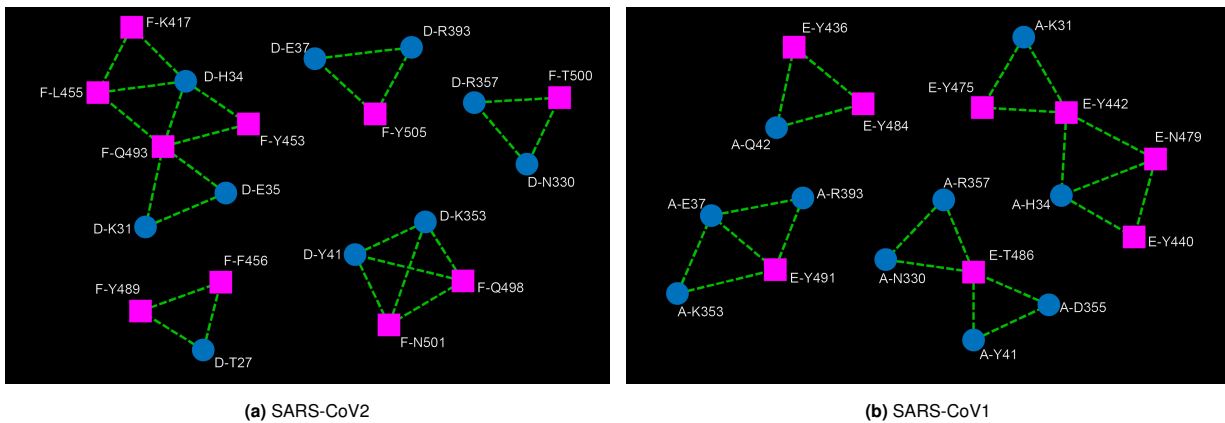
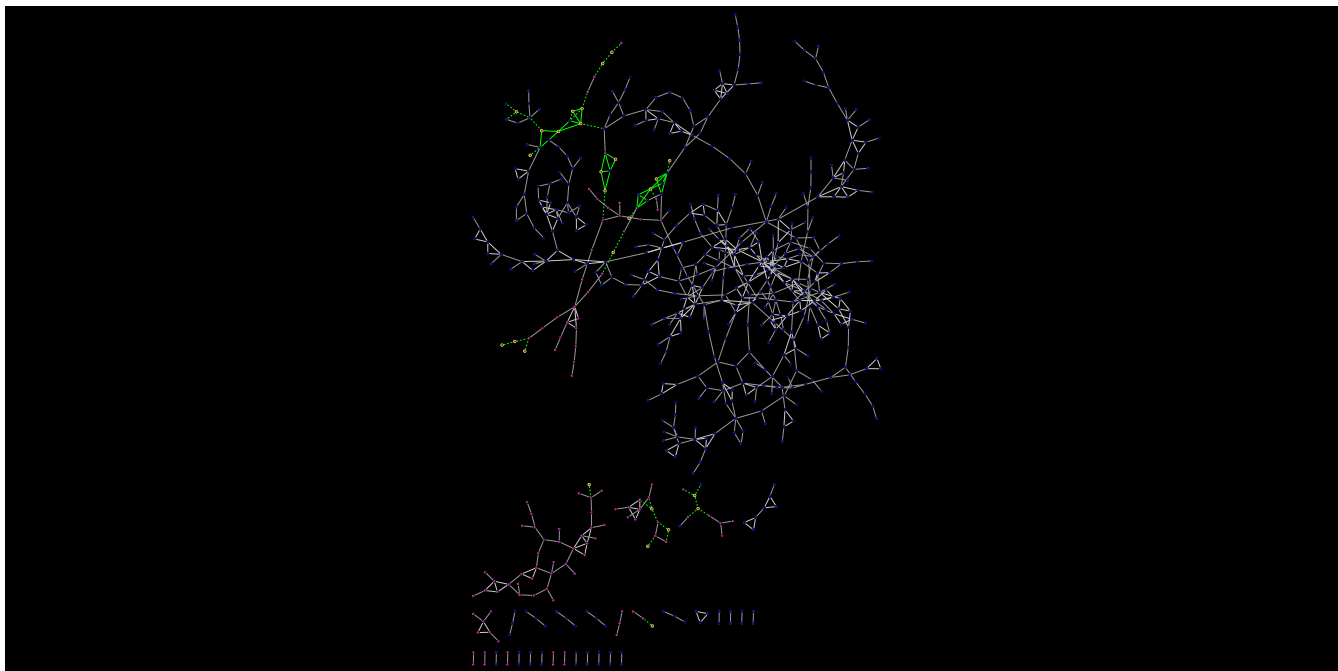
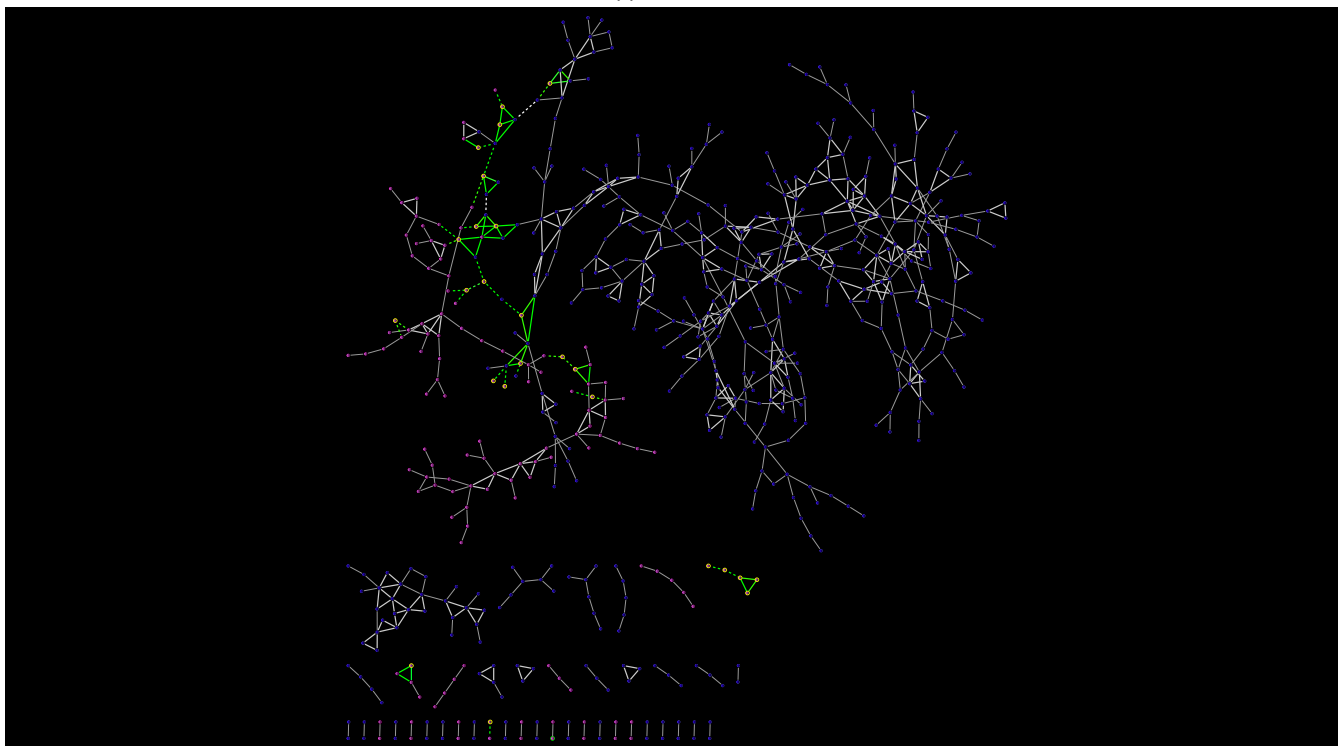


Fig. 3. The interface cliques obtained for the averaged network at I_{min} 2.75, 50% dynamic stability are presented here for the (a) SARS-CoV2 complex and (b) SARS-CoV1 complex. The residues/nodes corresponding to the ACE2 receptor are denoted as blue circles while those corresponding to the virus spike protein are denoted as magenta squares. Node labelling: First letter represents the Chain number in the PDB for each complex; The amino acid residues are shown in one letter code, followed by sequence number. The same representation is used in the Figures to follow.



(a) SARS-CoV1



(b) SARS-CoV2

Fig. 4. The largest cluster obtained for the averaged network at I_{min} 2.75, 50% dynamic stability are presented here for the (a) SARS-CoV1 complex and (b) SARS-CoV2 complex. The entire complex is represented by network metrics of edge, clique, community and cluster. The residues connected by green edges represent the interface nodes, and highlight the nature of their extended connection in the SARS-CoV2 complex as compared to the SARS-CoV1 complex. Non-interface cliques are shown in white color.

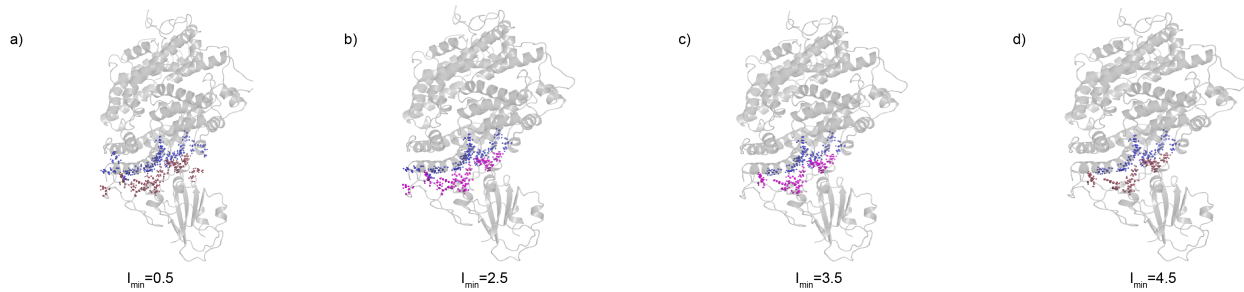


Fig. 5. The Pymol representation of the interface clusters of SARS-CoV1 complex at various I_{min} at 50% dynamical stability are presented here. The nodes corresponding to ACE2 receptor residues are represented in blue, while virus residues are represented in pink. The breaking up of the largest interface cluster for increasing values of I_{min} is indicative of the percolation-like behaviour highlighted in Fig.1. The SARS-CoV1 complex shows a reduction in the size of the interface cluster at $I_{min} \sim 2.5$ as corroborated in these representations.

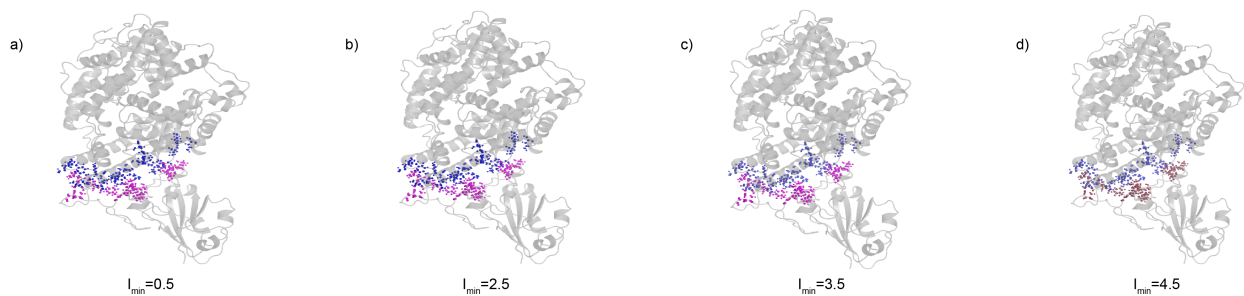
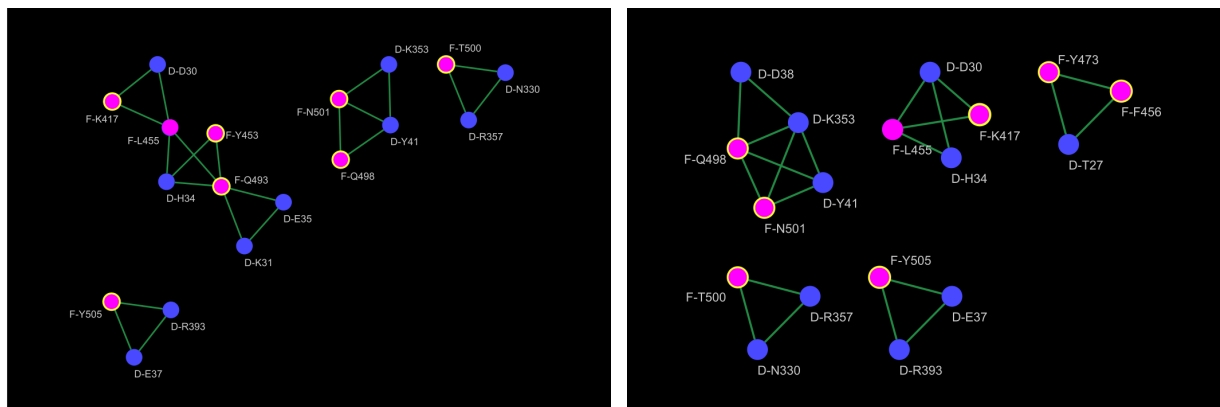
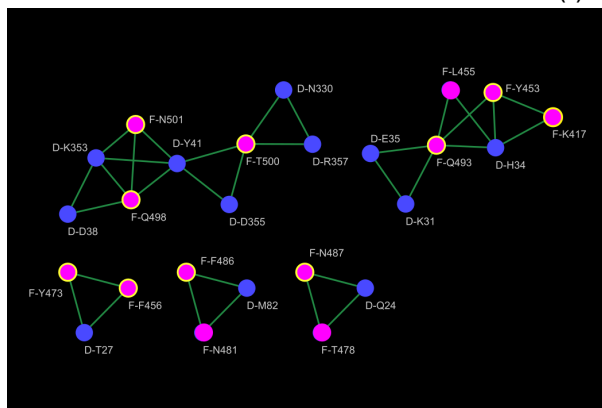


Fig. 6. The Pymol representation of the interface clusters of SARS-CoV2 complex at various I_{min} at 50% dynamical stability are presented here. The nodes corresponding to ACE2 receptor residues are represented in blue, while virus residues are represented in pink. The breaking up of the largest interface cluster for increasing values of I_{min} is indicative of the percolation-like behaviour highlighted in Fig.1. The SARS-CoV2 complex undergoes a more complex reduction in the size of the interface cluster, which persists up to $I_{min} \sim 3 - 3.5$ as corroborated in these representations. Thus, the interface cluster in this case persists for larger threshold values of edge interaction strength in comparison to SARS-CoV1.



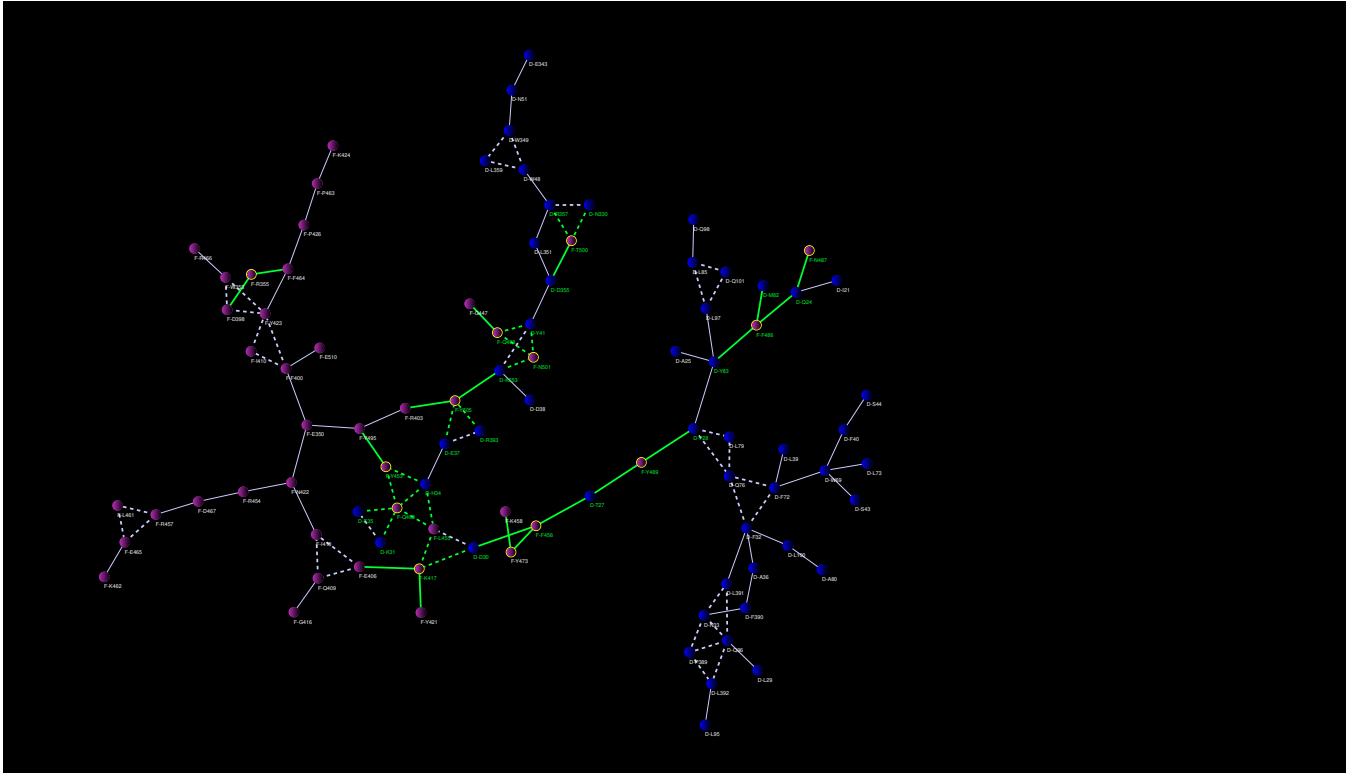
(a) Reference

(b) High RMSD

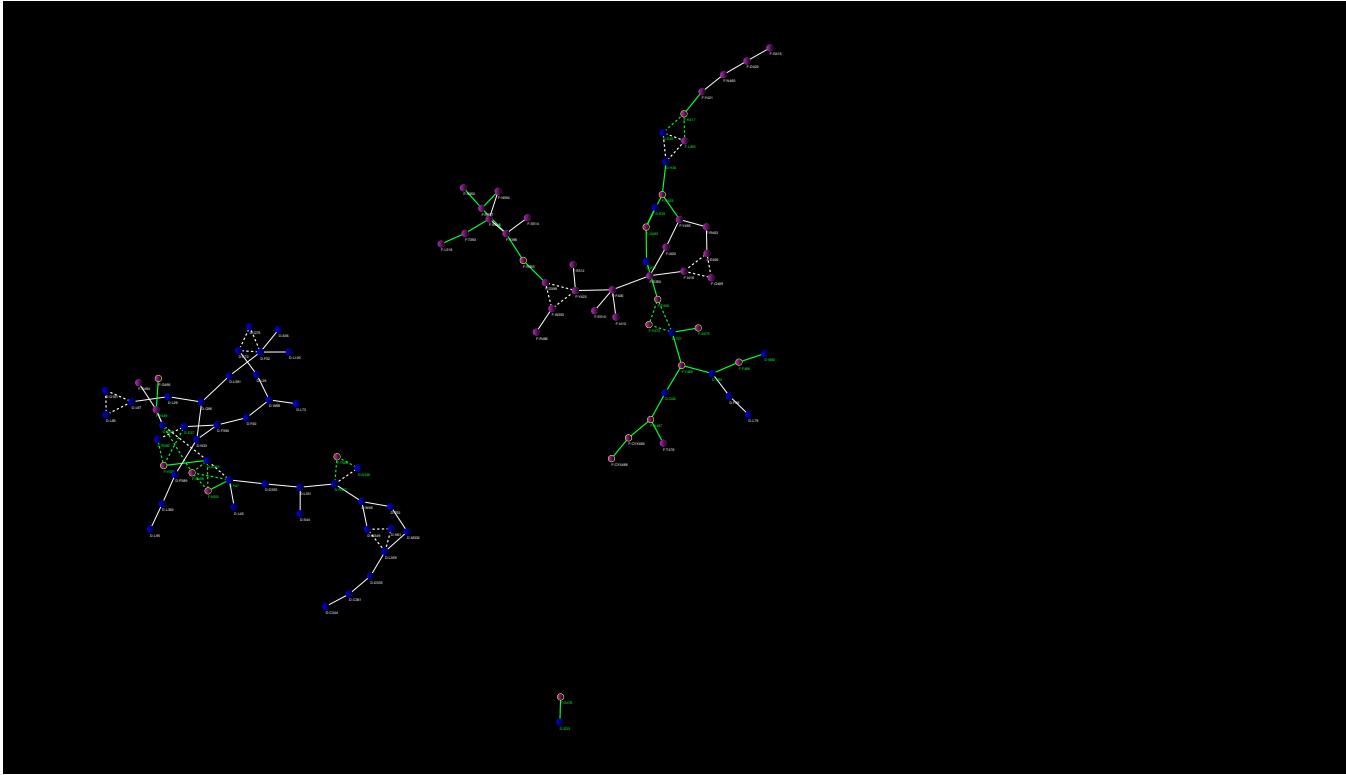


(c) End RMSD

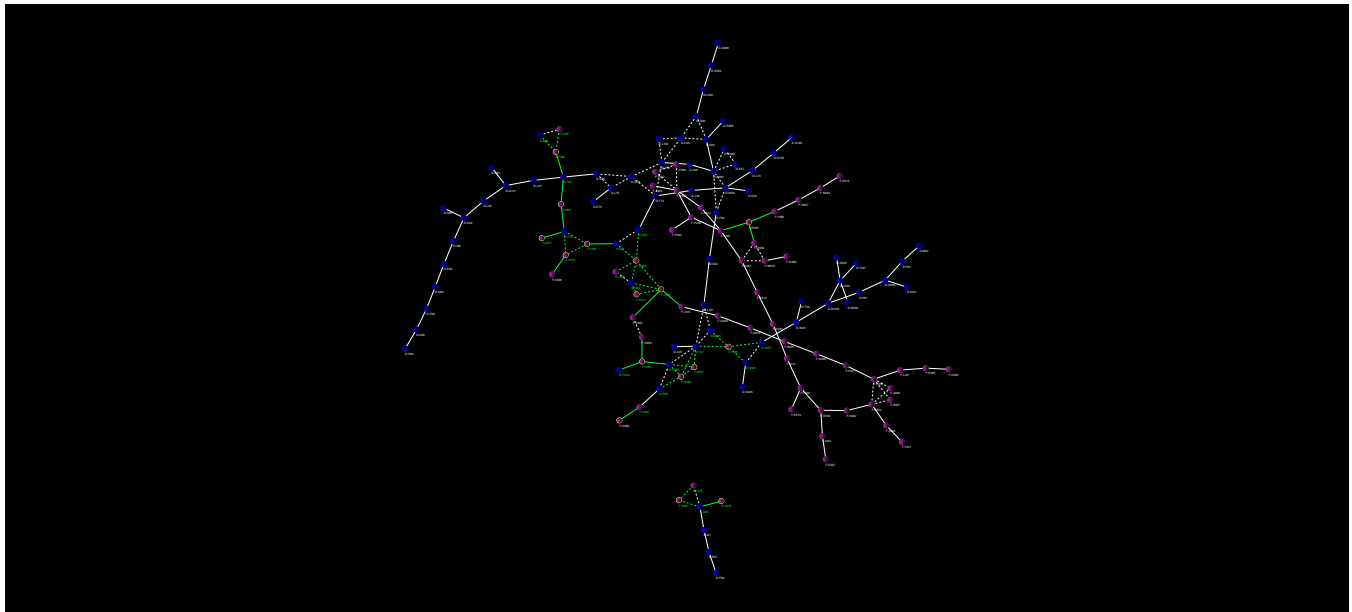
Fig. 7. The interface cliques/communities of the SARS-CoV2 complex in three selected snapshots ($J_{min} = 3.5$) are displayed here for the (a) Reference structure, (b) High RMSD and (c) End RMSD respectively. The mutated residues in variants are represented with a yellow outline on the nodes. The cliques obtained here as well as the nodes involved are similar to those obtained for the average network in Fig.3 but are significantly different highlighting the diversity of conformations explored during the simulation time.



(a) Reference Structure



(b) High RMSD Structure



(c) End RMSD Structure

Fig. 8. The interface clusters of the SARS-CoV2 complex in three selected snapshots ($I_{min} = 3.5$) are displayed here for the (a) Reference structure, (b) High RMSD and (c) End RMSD respectively. The residues connected by green edges represent the interface nodes.

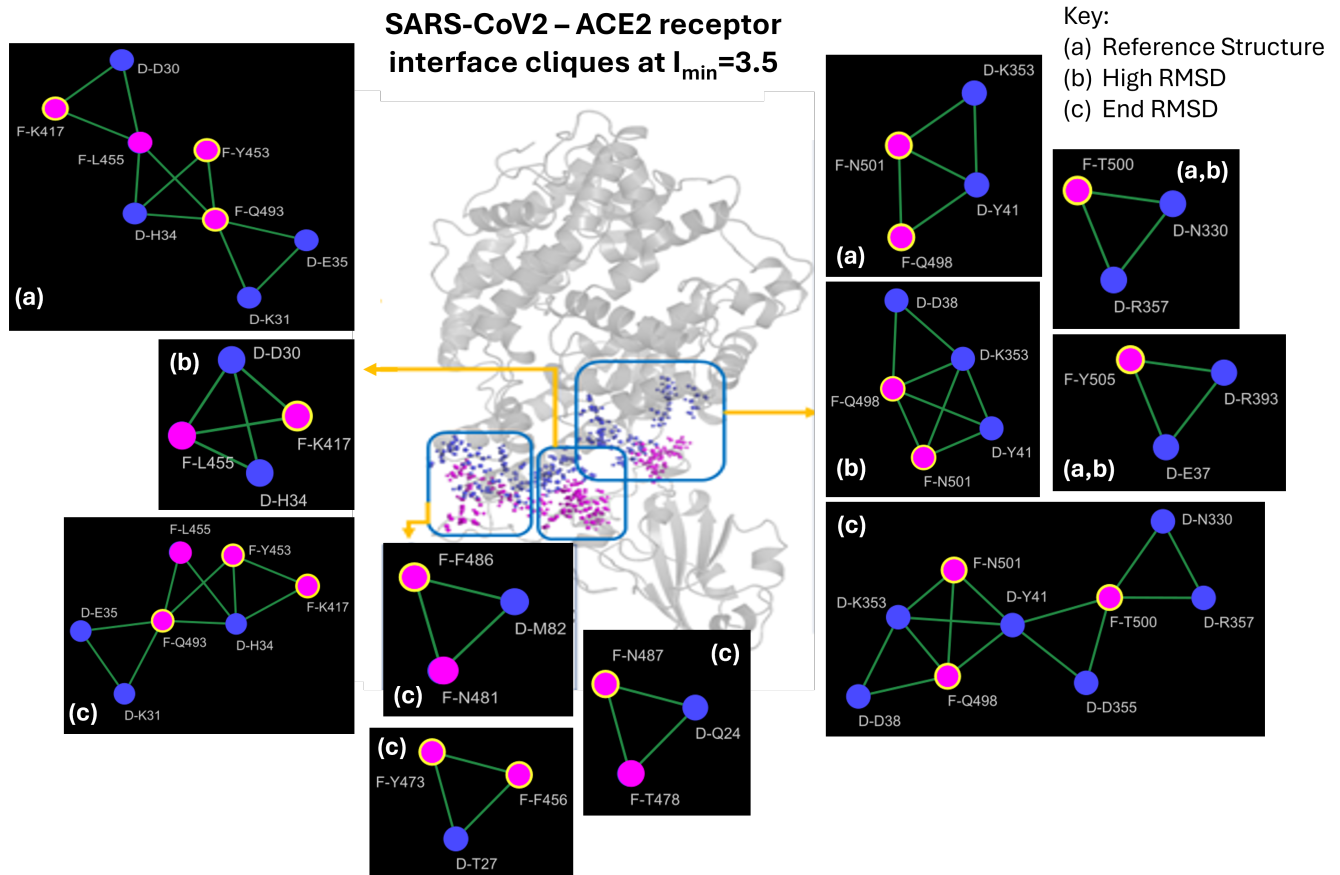


Fig. 9. The interface cliques in the three selected snapshots ($I_{min} = 3.5$) are represented over the PYMOL structure corresponding to the SARS-CoV2 complex, denoting their positions along the interface.

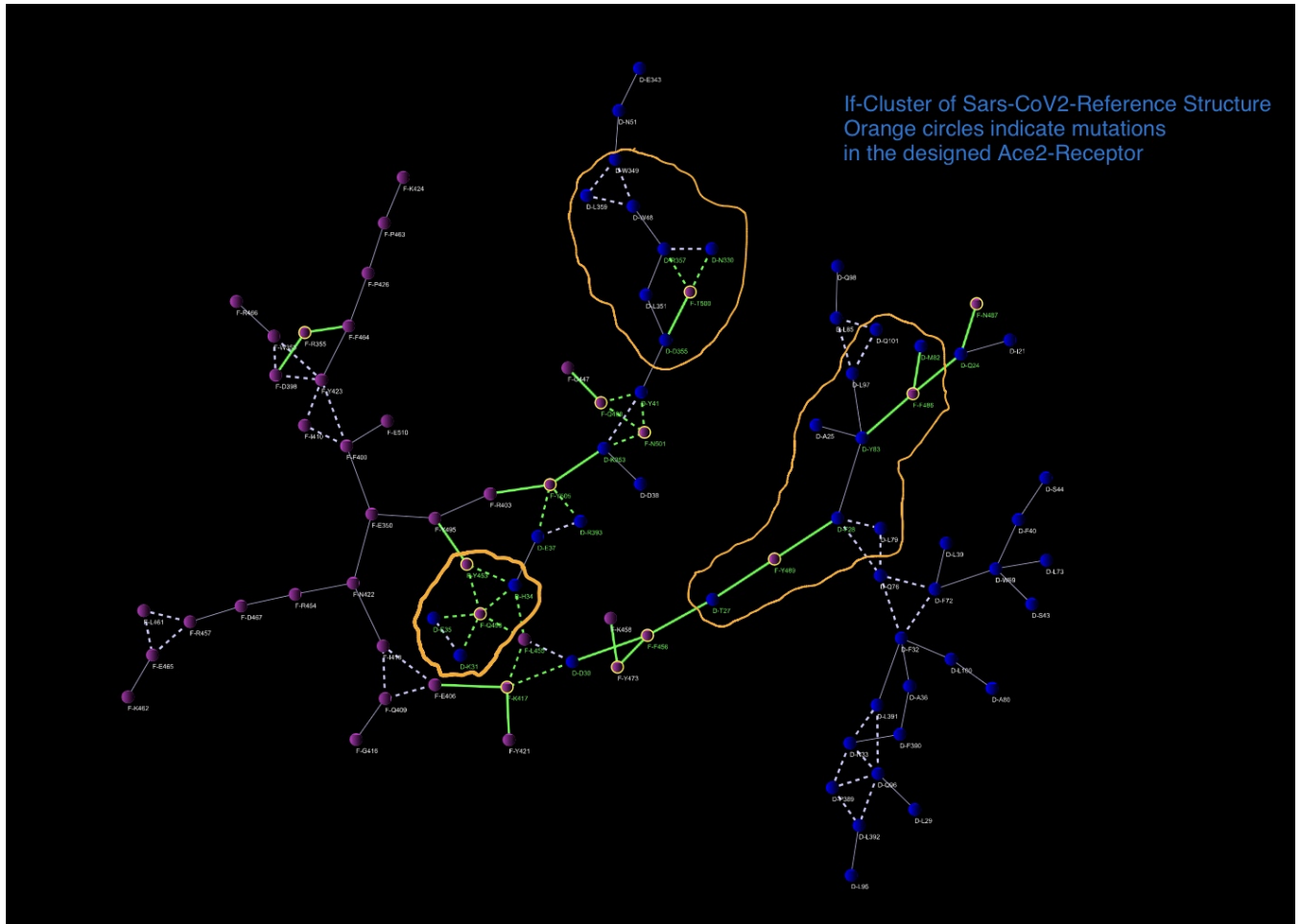


Fig. 10. Mutations in designed ACE2-Receptor are present in regions outlined by orange colour, which are represented on the interface cluster of the reference structure (Figure 8a)

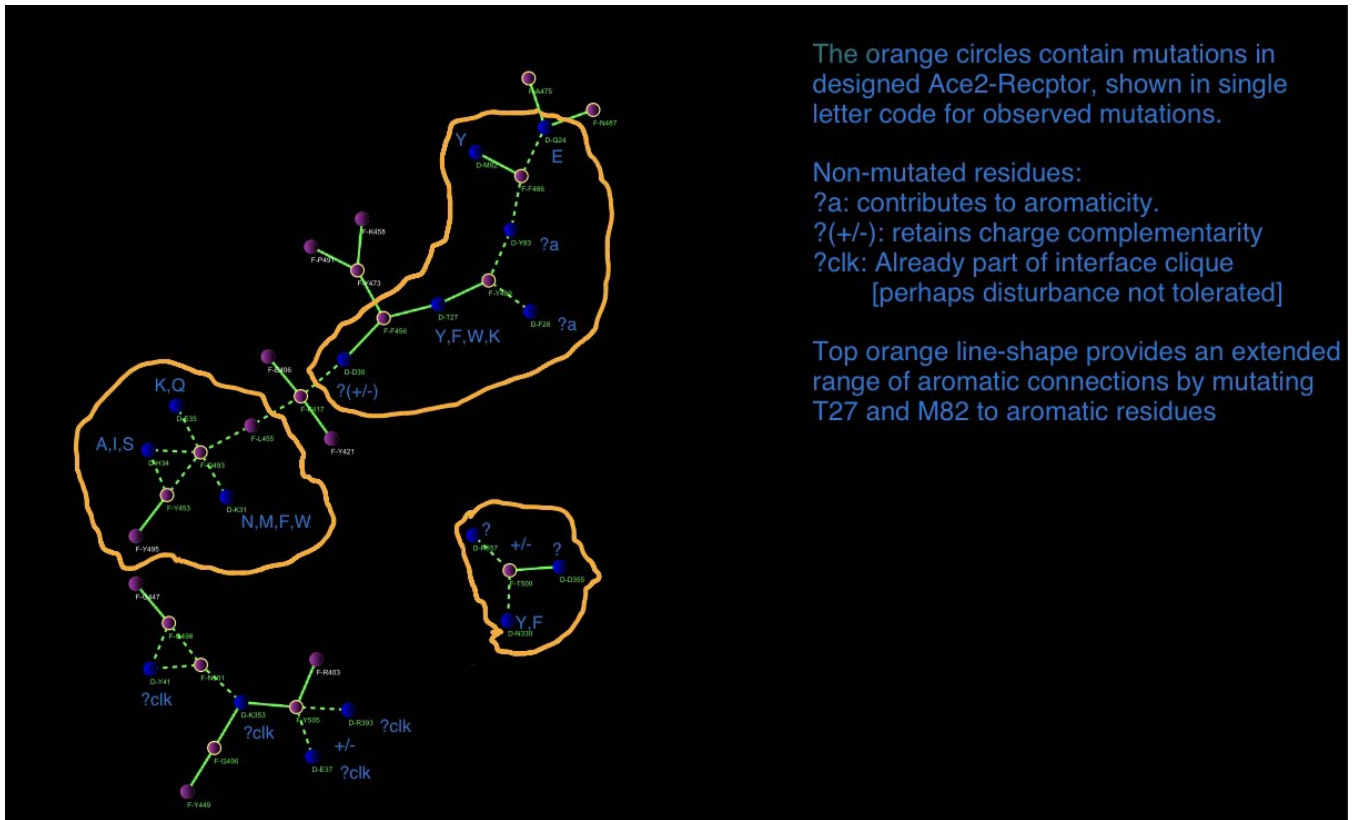


Fig. 11. The nodes in the ACE2-Receptor in the basic framework of the interface cluster, shown in Figure 10 are highlighted here. The physico-chemical characteristics of the mutated and non-mutated nodes are annotated. The mutated residues are represented with a yellow outline. Non-interface edges are represented by solid and dotted grey respectively. Among the non-mutated residues, we mark some of them with the following key - "?a" for residues that contribute to aromaticity, "?(+/-)" for those that retain charge complementarity and "?clk" for those residues that are already part of an existing clique. The orange loop thus shows an extended range of aromatic connections obtained by mutating T27 and M82 to aromatic residues.

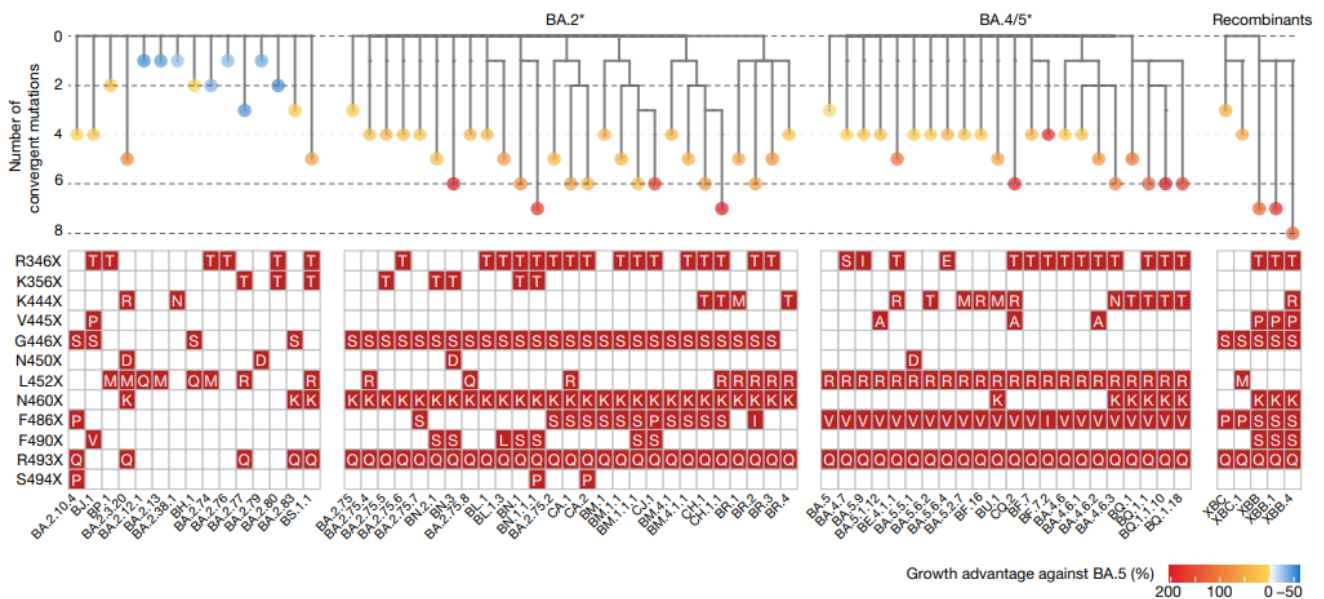
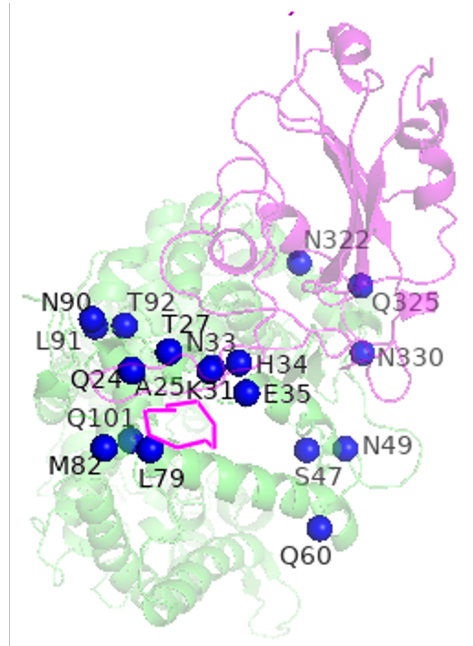


Fig. 12. Post Omicron evolutionary path of SARS-CoV2 lineages leading to complex-recombinant strains. This figure is reproduced as is from Reference (29) under a Creative Commons Attribution 4.0 International License (<http://creativecommons.org/licenses/by/4.0/>).



Q24(E)	A25(V)	T27(Y,F,W,K)	K31(N,M,F,W)	N33(D)	H34(A,I,S)	E35(K,Q)	L79(F,T)	M82(Y)	N90(D)
L91(P)	T92(Q)	Q101(H)	S47(A)	N49(E)	Q60(R)	N330(Y,F)	N332(Q)	Q325(Y)	

Fig. 13. The mutation sites for enhanced affinity in designing decoy ACE2 receptors are indicated in this figure. Possible residue substitutions are listed in the table below. The loop held by the disulphide bridge in SARS-CoV2 (Cys480-Cys488) is also highlighted as a pink ribbon. This figure is loosely adapted from Reference (35).

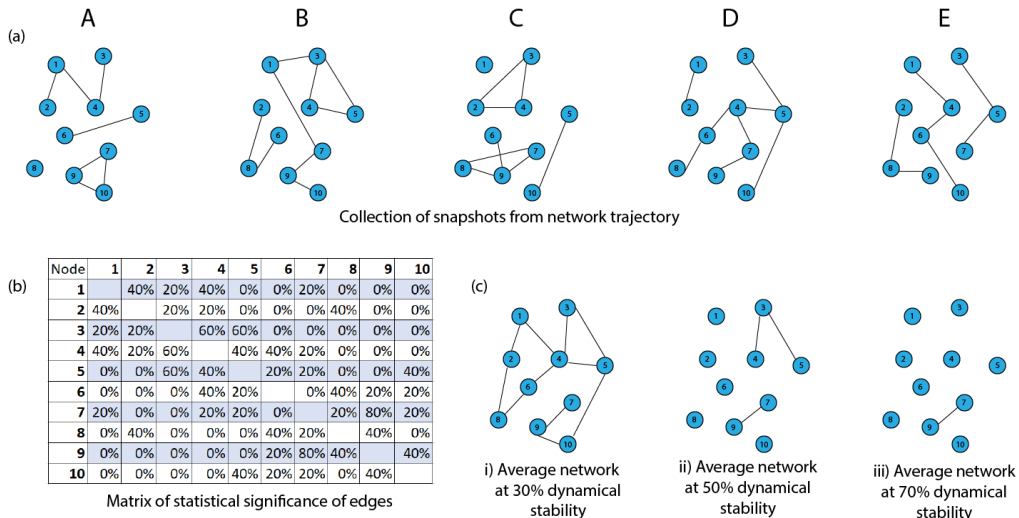


Fig. 14. The above figure offers a brief explanation for the concept of dynamic stability, which is a measure of statistical significance of a certain edge interaction over the entire period of simulation. We elucidate this idea using an example here. Consider a network whose edge interactions are being modified during the course of a certain amount of simulation time. Let the networks A-E in (a) be a collection of snapshots from this simulation trajectory. In (b), we represent the statistical significance of the edge between any two nodes in the network in the snapshots A-E as a matrix. That is, each entry in this matrix is the percentage of snapshots in which a particular edge is present. Here, dynamic stability is threshold value denoting the minimum statistical significance of each edge in the network. Therefore, the average network can be obtained given a certain value of dynamic stability. Such average networks for different values of dynamic stability are shown in (c).